Journal of Modern Materials
ISSN: 2456-4834
Volume 8, Issue 1, pp. 3-11, 2021
DOI: https://doi.org/10.21467/jmm.8.1.3-11

RESEARCH ARTICLE

Structure and New Substructure of α-Ti_2O_3: X-ray Diffraction and Theoretical Study

Soumia Merazka[1], Lamia Hammoudi[1] Mohammed Kars[1,2*], Mohamed Sidoumou[3], Thierry Roisnel[4]

[1] Faculté de Chimie, Laboratoire Sciences des matériaux, Université des Sciences et de la Technologie Houari-Boumediene, USTHB, Algérie.
[1, 2] Département de Chimie, Laboratoire Chimie Physique Moléculaire et Macromoléculaire (LCPMM), Université Blida1, Algérie.
[3] Département de Physique, Laboratoire de Physique Théorique et Interaction Rayonnement Matière, Université Blida1, Algérie.
[4] CNRS, ISCR (Institut des Sciences Chimiques de Rennes), Université de Rennes 1, France.

* Corresponding author email: mkarsdz@yahoo.fr

Received: 20 January 2021 / Accepted: 27 March 2021 / Published: 01 April 2021

ABSTRACT

The Crystal structure of both *a*-Ti_2O_3 and its new substructure with a halved c-axis has been investigated by single-crystal X-ray diffraction and density functional theory (DFT) calculations. The *a*-Ti_2O_3 substructure described in the R-3m space group, reveals an unusual 12-fold high coordination of Ti atoms forming edge and face-sharing distorted hexagonal prisms TiO_{12} stacking along the c-axis. The Hubbard-corrections predict a close bandgap for both α-Ti_2O_3 and its substructure; whereas a comparative study of their relative stability indicates that the substructure is thermodynamically less stable.

Keywords: Titanium oxide, CVT, X-ray diffraction, Crystal structure, Substructure, DFT.

1 Introduction

Titanium sesquioxide Ti_2O_3 belongs to the family of titanium oxide including various phases: TiO, TiO_2, Ti_3O_5, and the Magnéli phases Ti_nO_{2n-1} ($4 \leq n \leq 9$) [1, 2]. TiO_2 is the most important member due to its particular properties and commercial applications.

Recently, Ti_2O_3 has received a considerable amount of attention; One of the reasons for this, is that its ultranarrow bandgap (0.1 eV) [3, 4] allows it to be a promising candidate for potential photocatalytic applications. In fact, Ti_2O_3 (nanoparticles) can absorb solar energy in the full spectrum region and exhibits an excellent photothermal effect [5]. It's also considered a good candidate for long-wavelength mid-infrared (8-12 μm) photodetection.

Ti_2O_3 adopts the corundum *a*-Al_2O_3 type rhombohedral structural with space group of *R-3c* (N°167). Titanium atoms are located at 2/3 (two-third) of octahedral cavities of an approximate hexagonal close packing array of oxygen atoms [6]. With increasing temperature, structure refinement of *a*-Ti_2O_3 shows significant variations in the lattice parameters. These changes are associated with a semiconductor to a semi-metal phase transition, and primarily due to the change in the c-axial Ti-Ti bond distances [7, 8].

Under pressure, a theoretical study of oxygen-rich Ti-O compounds by Zhong *et al.* [9, 10] predicted various structures with remarkable features: high coordination of Ti atoms is expected in TiO_2 (> 690 GPa) and in TiO_3 (> 179 GPa) with a 10-fold and 12-fold Ti-O coordination respectively. In the Ti_2O_5 (> 131 GPa), the 10-fold coordination of Ti atoms is associated with the presence of peroxide group (O_2^{2-}) with single bond O-O of oxygen.

Herein, a substructure of *α*-Ti_2O_3 with a halved *c*-axis (c/2) was accidentally synthesized by CVT (Crystal Vapor Transport) in the course of an experiment in the system Ge-Sb-Ti.

Crystal structure of *a*-Ti_2O_3 and its new substructure were investigated by a combined experimental and computational investigation by means of single crystal X-ray diffraction and DFT calculations using the Cambridge Sequential Total Energy Package Code (CASTEP). The main distinction between the *a*-Ti_2O_3 structure and the substructure are also discussed.

The sesquioxide Ti_2O_3-substructure reveals an unusual 12-fold high coordination of Ti atoms (the highest coordination number among all Ti-O compounds known so far) forming distorted hexagonal prisms TiO_{12} that was predicted to exist in Ti/O compounds only at high pressure.

2 Research Methodology

2.1 Crystal growth and chemical analysis

Single crystals of Ti_2O_3 and its substructure were accidentally obtained by CVT during our attempts to prepare ternary Ge-Sb-Ti. Two mixtures of pure elements in a ratio 1:2:5 were sealed into an evacuated quartz tube with I_2 + WO_3 to favour the crystallization. The mixtures between 950-980 °C (batch 1) and 1000-1030 °C (batch 2) respectively were heated for one month, then slowly cooled to room temperature. Purple platelet-like crystals with rough surface were grown in the cold end of the tubes.

The morphologies and chemical compositions of the samples were analyzed by scanning electron microscopy (SEM, FEI Quanta 650 FEG) images and energy-dispersive X-ray spectroscopy (EDS) spectra (Figure S1). The results indicated an approximate ratio of 2:3 for Ti and O [Ti (at. %) = 44.13 and O (at. %) = 55.87].

2.2 Single crystal structure determination

Single crystals data were collected using an APEXII CCD and a D8 VENTURE PHOTON 100 X-ray diffractometer (Bruker AXS) with graphite-monochromated Mo Kα radiation.The reflection intensities were integrated with the SAINT [11]. Absorption correction was applied by SADABS [12]. The crystal structures were solved using the program Superflip [13] and refined by using the program JANA2006 [14]. Experimental details are given in Table1.

Table 1: *Selected single crystal data and structure refinement parameters for the α-Ti_2O_3 and α-Ti_2O_3 substructure*

	α-Ti_2O_3 (150K)	α-Ti_2O_3 (293K)	α-Ti_2O_3 sub (293 K)
Formula	$Ti_{1.935}O_3$	$Ti_{1.951}O_3$	$Ti_2O_{3.096}$
Molar mass ($g.mol^{-1}$)	140.6	141.4	145.3
Space group	*R-3c*	*R-3c*	*R-3m*
Z	6	6	3
Unit cell dimensions (Å)	*a* = 5.1631(8) *c* = 13.584(2)	*a* = 5.1788(4) *c* = 13.6525(12)	*a* = 5.1789(4) *c* = 6.8260(6)
Volume ($Å^3$)	313.60(9)	317.10(4)	158.55(2)
Calculated density ($g.cm^{-3}$)	4.467	4.4416	4.5635
Absorption coefficient (mm^{-1})	7.073	7.051	7.229
Angular range *Θ*(°)	5.46- 40.11	5.44-45.39	5.44 - 45.21
Index ranges	-9<*h*<9 / -8<*k*<9 -24<*l*<24	-10<*h*<9 / -9<*k*< 10 -26<*l*<18	-10<*h*<9 / -9<*k*<10 -13<*l*<9
R_{int}	0.0579	0.032	0.0311
Total recorded reflections	1521	2936	1324
Independent reflections	236	504	307
Reflections with $I > 3\sigma(I)$	225	465	295
T_{min}/T_{max}	0.4001/0.7479	0.4491/0.7489	0.4513/0.7489
Data	12	12	12
Goodness-of-fit on F^2	2.03	1.81	1.73
$(R/R_w)_{obs}$ (%)	0.0330/ 0.0422	0.0218/ 0.0325	0.0204/ 0.0276
$(R/R_w)_{all}$ (%)	0.0336/ 0.0425	0.0231/ 0.0331	0.0209/ 0.0278
$\Delta\rho_{max}$, $\Delta\rho_{min}$ ($e^-/Å^3$)	1.83, -2.51	0.75, -1.96	1.14, -1.14

The crystals of Ti_2O_3 under investigation were obverse/reverse twinned, with a refined twin domain fraction of 0.364 (3): 0.636 (3) at 150 K and 0.3359 (16): 0.6641 (16) at 293 K.

All the atoms in the α-Ti_2O_3 structures and substructure were refined anisotropically in the final cycles of the refinement. Tables S1, S2, and S3 of the Supplementary material report atomic coordinates, anisotropic displacement parameters, and selected bond distances.

The deposition numbers CCDC 2055781-2055787-2055825 contains the supplementary crystallographic data for this paper. These data can be obtained free of charge via www.ccdc.cam.ac.uk/conts/ retrieving.html (or from the Cambridge Crystallographic Data Centre, 12 Union Road, Cambridge CB2 1EZ, UK; fax: (+44) 1223-336- 033; or deposit@ccdc.ca.ac.uk).

2.3 Theoretical calculations

All calculations of the α-Ti_2O_3 and its substructure were conducted using DFT calculations as implanted in the CASTEP code [15] which is one of the software modules in Materials Studio [16]. The electron exchange-correlation potential is calculated within the generalized gradient approximation as described by Perdew, Burke, and Ernzerhof (GGA-PBE) [17] while the ultrasoft pseudopotential method is used to explain the interactions between the ion core and the valence electrons. The cut-off energy was set at 340 eV while, in the Brillouin zone, the Monkhorst–Pack scheme [18] was sampled with 7x1x1 K-point mesh. For the atomic pseudopotential calculation of Ti and O, the valance electronic configurations considered were respectively $3p^6 3d^2 4s^2$ and $2s^2 2s^4$.

In order to compare the relative stabilities of *a*-Ti_2O_3 and its substructure, the experimental crystallographic data obtained from X-ray diffraction studies at ambient temperature (293 K) were used in all calculations with fixed unit cell parameters at their experimental values. The GGA+U with U = 2.5 eV scheme was adopted to include the correlations effects in the Ti 3d shell into account.

The formation energy ΔE was calculated at 0 K for both the structure and the substructure according to the following equation:

$$\Delta E = \frac{1}{(x+y)}\left[E_{DFT} - xE_{Ti} - yE_O\right]$$

where the total energy of Ti_2O_3 (structure or substructure) is expressed by E_{DFT}, E_{Ti} and E_O which represent the titanium and oxygen potentials calculated in their respective bulks, and x and y which represent the number of Ti and O atoms, respectively.

3 Results and Discussion

The crystals of Ti_2O_3 selected from batch 1 (collected at 150 K), correspond to the corundum *a*-Al_2O_3 type structure with lattice parameters a = b = 5.1631 (8) Å and *c* = 13.584 (2) Å, and space group *R-3c* (N°167). In the structure, the basic building block consists of octahedrons TiO_6, sharing one face and three edges (Figure 1). The bond distances are comparable to those observed in other structures refinement by some authors [7, 19-21]. The Ti-O distances range from 2.0271 (14) to 2.0661 (16) Å, Ti atoms are then shifted from the centre of the octahedron, to minimize the Ti-Ti [2.5668 (10) – 2.9963 (13) Å] interactions. The structure refinement gives rise to the formula $Ti_{1.935}O_3$, with refined site occupancy of Ti about 97(2) %.

Bragg reflections of crystals selected from batch 2 (collected at ambient temperature), could be indexed correctly based on two rhombohedral unit cells: the α-Al_2O_3 type structure with lattice parameters *a* = *b* = 5.1788 (4) Å and *c* = 13.6525 (12) Å and its subcell with halved *c*- axis, *c/2* (a = *b* = 5.178 (4) Å and *c* = 6.8260 (6) Å). It was observed that the mean intensities *I/sig (I)* of *hkl* reflections with *l* being an odd number is very weak (twice weaker) than those with *l* even, suggesting a substructure of corundum with a periodicity of *c/2*.

The substructure was solved by Superflip [13], the best results were obtained with the model in the space group *R-3m* (N°166); a minimal non-isomorphic supergroup of *R-3c* space group. *R-3c* represents a maximal k non-isomorphic subgroup of the space group *R-3m*. The group-subgroup relationship leads to a klassengleich symmetry reduction of index 2 (Figure S2).

The observed Ti-O, O-O and Ti-Ti distances ranging from 2.0347 (13) - 2.0729 (11) Å, 1.6207(17) - 2.2826 (4) Å and 2.5847 (2) – 3.0060(2) (13) Å respectively, are close to those observed in the *a*-Ti_2O_3 (see Table S3).

The structure refinement of α-Ti_2O_3 substructure gives rise to the formula $Ti_2O_{3.097}$ close to the ideal formula Ti_2O_3. The refined site occupancy of O is about 51.6%, this suggests that the structure of *a*-Ti_2O_3 results from the ordering of oxygen atoms along the *c*-axis.

The most important feature of the *a*-Ti_2O_3 substructure is the unusual 12-fold coordination of Ti atoms with oxygen. However, this is uncommon and the highest Ti-O coordination, which was predicted only theoretically to occur at high pressure in TiO_3 [10] was experimentally observed in the $LiInTi_2O_6$ compound [22].

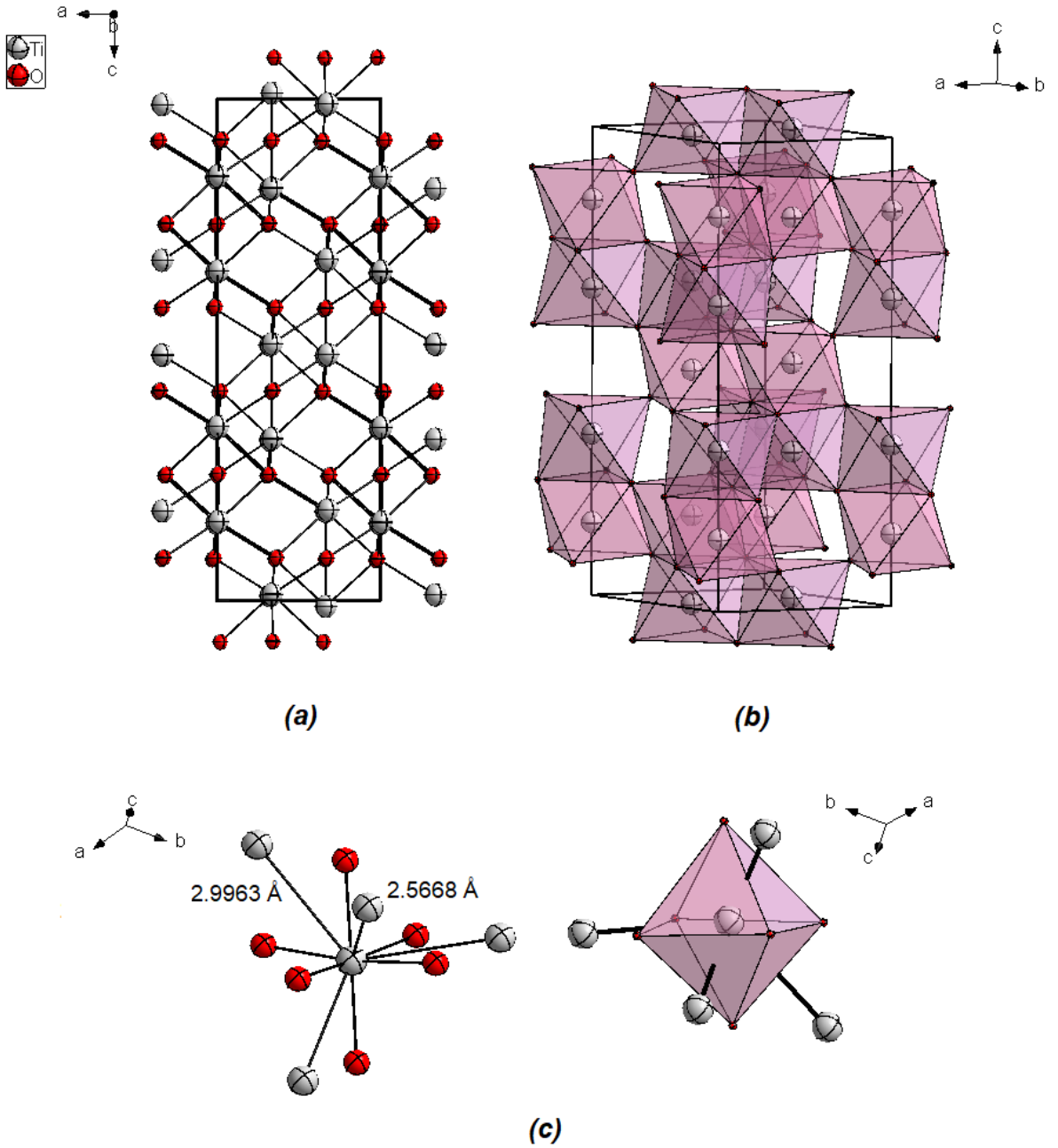

Figure 1: *Crystal structure of α-Ti_2O_3: (a) projected along the c axis including 95% probability displacement ellipsoids. (b) Clinographic view of face and edges sharing TiO_6 octahedrons. (c) Distorted octahedral coordination around Ti metal atoms showing the short Ti-Ti distance*

The substructure consists of a three-dimensional framework of distorted hexagonal TiO_{12} prisms connected by edge and face sharing and stacking along the c-axis (Figure 2(b)).

Figure 2(d) represents a two-dimensional framework of the substructure along the c-axis, with honeycomb holes created by layers of TiO_{12} polyhedrons sharing three side faces at 120° angles. Compared to the α-Ti_2O_3 substructure, the TiO_{12} polyhedrons in $LiInTi_2O_6$ are more distorted; the Ti-O distances range from 1.7946 - 2.1201 Å, while the O-O bonds are shorter 1.437 - 1.980 Å. In fact, the structure of $LiInTi_2O_6$ (space group *R-3m*), can be considered as another superstructure of the α-Ti_2O_3 substructure (space group *R-3m*), which can be derived by a double klassengleich symmetry reduction of index 2 (see Figure S2). Indeed, a full occupancy of Ti atoms in the mixed positions of In/Li/Ti results in the formula Ti_4O_6 (ie) Ti_2O_3.

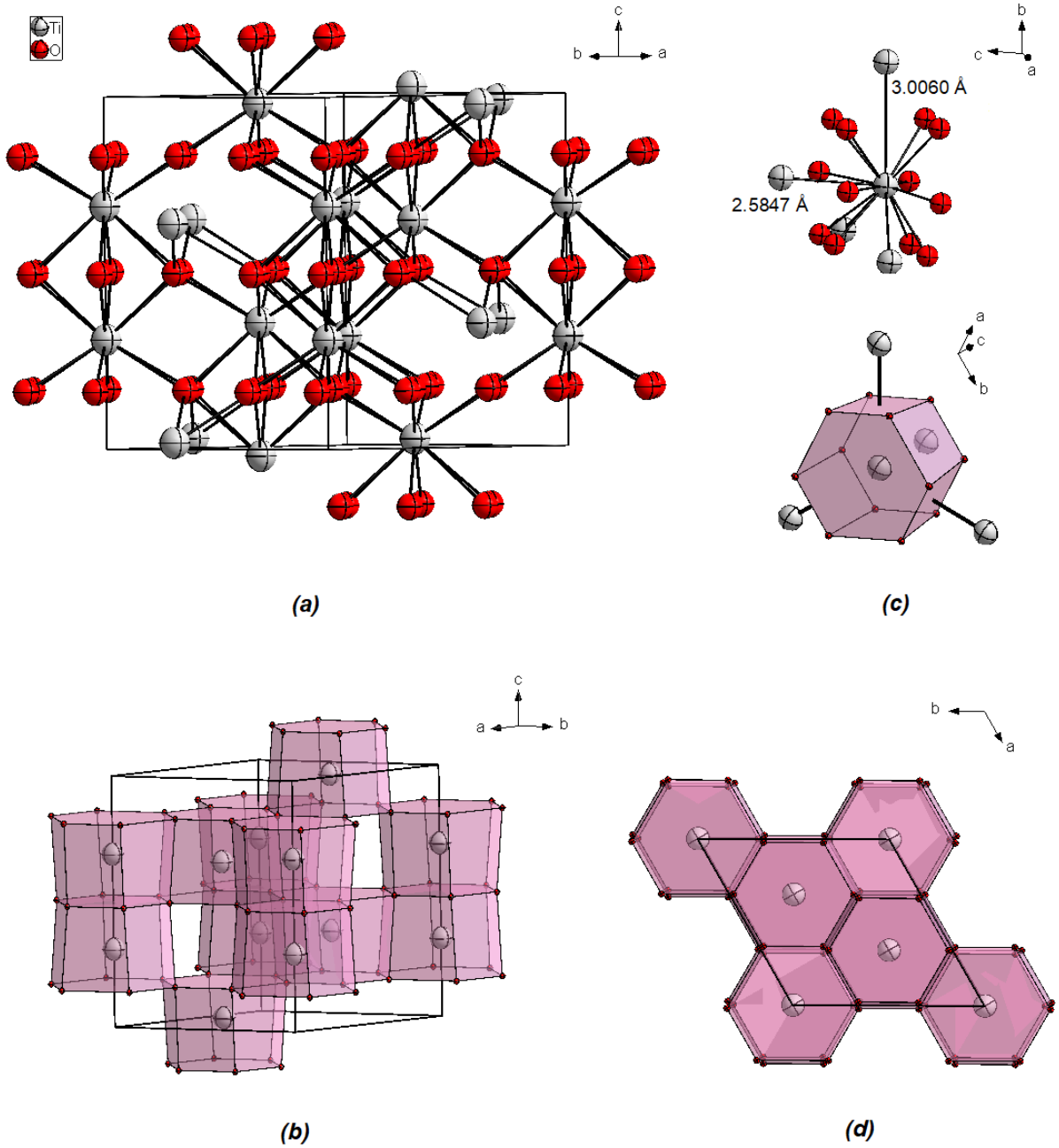

Figure 2: *Crystal structure of α-Ti_2O_3 substructure: (a) projected along the c axis including 95% probability displacement ellipsoids. (b) Clinographic view of faces TiO_{12} polyhedrons. (c) Distorted polyhedron coordination around Ti metal atoms showing the short Ti-Ti distance. (d) 2D-two dimensional framework of the substructure along the c axis with honeycomb holes created by layers of TiO_{12} polyhedrons*

Table 2: *Mulliken population analysis, Bandgap (eV), and calculated formation energy ΔE (eV) for both structure and substructure of α-Ti_2O_3.*

Phases	Species	s	p	d	Total	Charge (e)	Bond	Length (Å)	Population	Bandgap	ΔE
α-Ti_2O_3	O	1.84	4.87	0.00	6.71	-0.71	Ti-O	2.0340/2.0739	0.30 /0.27	0.135	-4.67
	Ti	2.28	6.38	2.28	10.94	+1.06	Ti-Ti	2.5851/3.0060	-0.15 /-0.86		
α-Ti_2O_3-sub	O	1.90	4.52	0.00	6.42	-0.42	Ti-O	2.0346	0.21	0.175	-1.86
	Ti	2.25	6.20	2.28	10.72	+1.27	Ti-Ti	2.5847	-1.74		

It should be noted, that the unit cell constants of the α-Ti_2O_3 structure collected at ambient temperature (293 K) are somewhat larger than reported in the literature by many authors (Table 1). These deviations may reflect certain differences in stoichiometry and purity of the synthesis corundum. On the other hand, an increase in most structural parameters is observed as compared to the *a*-Ti_2O_3 structure collected at low temperature (150 K).

Indeed, during corundum heating between 296 K and 390 K, Rice and Robinson [7] also reported a small increase in these structural parameters. However, structural changes above that temperature are nonlinear up to 868 K. The structures refinement at both 150 and 293K, suggests a deficit in the Ti positions. A defect model seems to occur by introducing vacancy (about 3%) in order to minimize the interactions between Ti-Ti pairs.

Otherwise, a correlation seems to exist between the calculated Bond-valence-sum BVS [23] of Ti atoms and the Ti-Ti distances, indicating that a mixed-valence Ti^{+3}/Ti^{+4} are required for a charge balance (see Table S3). Such kind of adjustment between BVS and Ti-Ti distances was also observed in some Magnéli phases [24].

Theoretical calculations of both structure and substructure of *a*-Ti_2O_3 are listed in Table 2. It is noteworthy that the calculated formation energy of Ti_2O_3-subcell is smaller than zero, suggesting that this substructure is thermodynamically stable, but obviously, the α-Ti_2O_3 structure is thermodynamically more stable.

Figure 3 shows the band structures and density of states (PDOS) of both α-Ti_2O_3 structure and α-Ti_2O_3 substructure. Local functional GGA gives a metallic band structure (without band gap) for α-Ti_2O_3 [25, 26] and its substructure as expected. Notably, our results were improved and a gap opens-up using the Hubbard corrections with *U* = 2.5 eV [27], the calculated α-Ti_2O_3bandgap of about 0.135 eV (Figure 3 (a)) is close to the experimental value of 0.1 eV [28] while the substructure bandgap slightly increases to 0.175 eV (Figure 3 (b)). On the other hand, the calculated bandgap using the hybrid functional HSE06 predicts much greater values around 1.4 eV.

The PDOS (Figure S3), shows that the occupied state's region below the Fermi level E_F of 02 phases under investigation are mainly contributed by O-2p with a small admixture of the Ti-3d states whereas the high energy part consists of Ti-3d states. Unlike the substructure, the valence band, which extends from 8 eV, is separated into two regions by a bandgap of about 2 eV in the corundum structure.

Furthermore, Mulliken population analysis was performed using the CASTEP package to quantify the charge transfer and evaluate the chemical bond for the two systems. One can see clearly from Table 2, the electron charge transfer from the Ti atoms to the O atoms. The bond population for Ti-O ranges from 0.21 to 0.30 indicating a low degree of covalency whereas the Ti-Ti bond population ranging from -0.15 to -1.74 indicates a state of non-interaction or anti-bonding. Indeed, the value near zero is for ionic bond characters and the value greater than zero measures the degree of covalency while the negative value indicates anti-bonding interaction. The bond population for Ti-O in the substructure is lower compared to the *a*-Ti_2O_3 structure, that in Ti-Ti are the most anti-bonding, suggesting a less stable substructure and corroborating the CASTEP calculated formation energy.

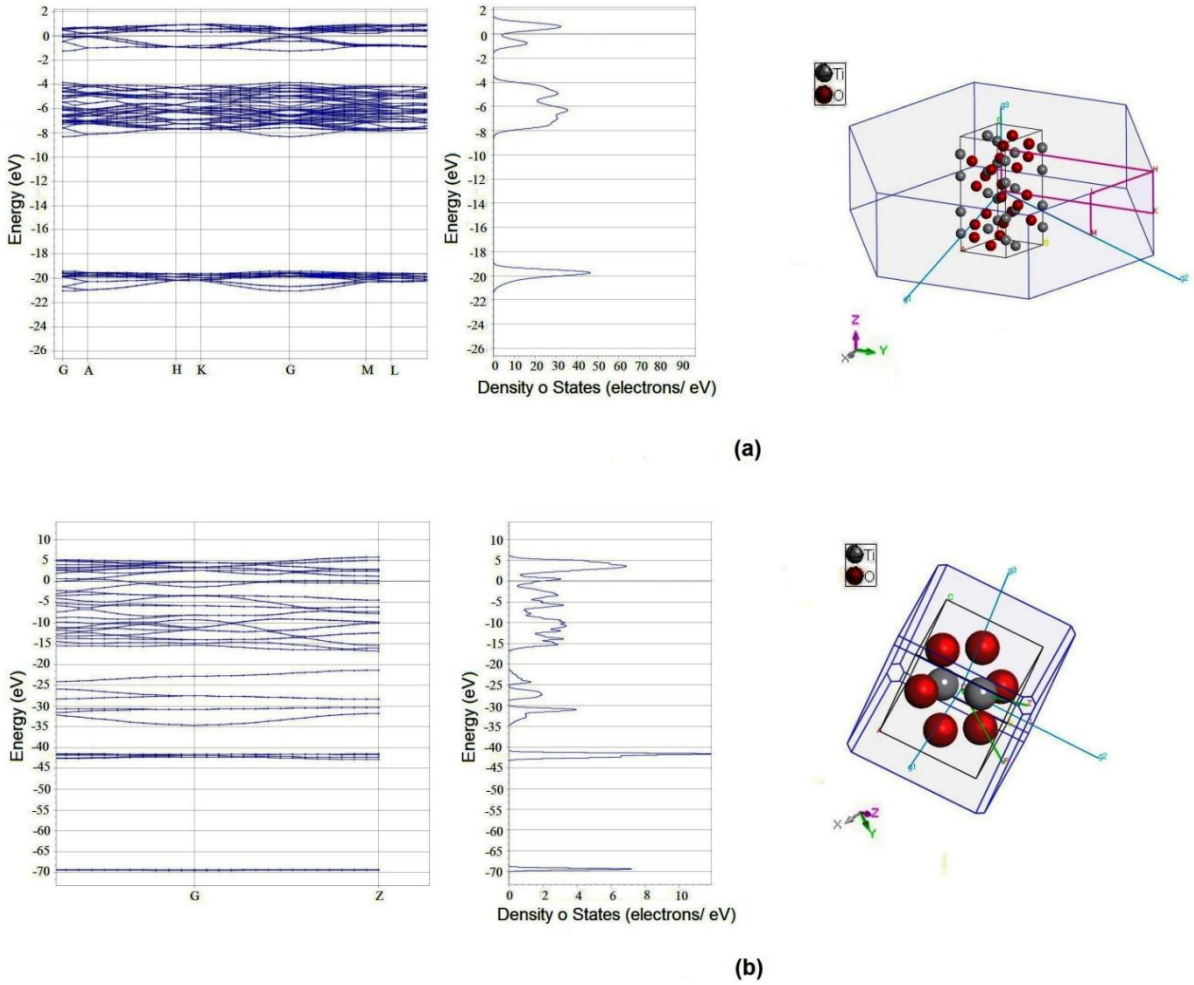

Figure 3: *Electronic band structure and their corresponding DOS, Brillouin zone with high-symmetry points labeled: (a) α-Ti_2O_3; (b) α-Ti_2O_3 substructure*

4 Conclusions

In this paper, a new substructure of α-Ti_2O_3 with a halved *c*-axis was synthesized by CVT and revealed by single crystal X-ray diffraction. The experimental results of both *a*-Ti_2O_3 and its substructure were supported by theoretical calculations. The substructure consists of a three-dimensional framework built by packing edge and faces sharing distorted TiO_{12} hexagonal prisms along the *c*-axis and reveals an unusual 12-fold high coordination of Ti atoms. The partial site occupancy of O, suggests that the *a*-Ti_2O_3 structure results from the substructure by ordering the oxygen atoms along the *c*-axis. The band structure calculation by CASTEP code using the Hubbard-corrections for α-Ti_2O_3 is about 0.135 eV, close to the experimental value of 0.1 eV, whereas the substructure bandgap increases slightly to 0.175 eV. It is noticeable that the calculated formation energy of Ti_2O_3-subcell indicates a stable thermodynamically substructure but clearly less stable than the *a*-Ti_2O_3 structure.

5 Supplementary Contents

The following supplementary contents are available at URL https://journals.aijr.in/index.php/jmm/article/view/3489/382

Table S1: *Atomic coordinates and equivalent isotropic displacement parameters (Å²) for α-Ti_2O_3 (150 K), α-Ti_2O_3 (293 K) and α-Ti_2O_3 substructure (293 K)*

Table S2: *Anisotropic displacement parameters for α-Ti_2O_3 (150 K), α-Ti_2O_3 (293 K) and α-Ti_2O_3 substructure (293 K)*

Table S3: *Selected bond distances (Å) and Bond valence calculation (BVS) for α-Ti_2O_3 (150 K), α-Ti_2O_3 (293 K) and α-Ti_2O_3 substructure (293 K)*

Figure S1: *Typical SEM-EDS spectra obtained on single crystals of the α-Ti_2O_3 samples*

Figure S2: *The group-subgroup relationship between: the structure of the α-Ti_2O_3, the α-Ti_2O_3 substructure and $LiInTi_2O_6$ structure. The indices for the translationengleiche (t) transition and the site symmetries of the Wyckoff sites are given*

Figure S3: *Partial DOS of: (a) α-Ti_2O_3; (b) α-Ti_2O_3 substructure*

6 Competing Interests

There is no potential conflict of interest exists in this publication.

How to Cite this Article

S. . Merazka, L. . Hammoudi, M. Kars, M. . Sidoumou, and T. . Roisnel, "Structure and New Substructure of α-Ti2O3: X-ray Diffraction and Theoretical Study", *J. Mod. Mater.*, vol. 8, no. 1, pp. 3-11, Apr. 2021.

References

[1] J. L. Murray and H. A. Wriedt. The O-Ti (Oxygen-Titanium) system. *J. Phase Equilib*, Vol 8, pp. 148-165, 1987. https://doi.org/10.1007/BF02873201

[2] H. Okamoto. O-Ti (Oxygen-Titanium). J. Phase Equilib. Diffus, Vol 32, pp. 473, 2011. https://doi.org/10.1007/s11669-011-9935-5

[3] H. Nakastsugawa and E. Iguchi. Transition phenomenon in Ti_2O_3 using the discrete variational X α cluster method and periodic shell model. *Phys Rev*, Vol B56, pp. 12931-12938,1997 https://doi.org/10.1103/PhysRevB.56.12931

[4] Y. Li. Weng, X. Yin, X. Yu, S. R. S. Kumar, N. Wehbe, H. Wu, H. N. Alshareef, S. J. Pennycook, B. H. B. Breese, J. Chen, S. Dong and T. Wu. Orthorhombic Ti_2O_3: A Polymorph-Dependent Narrow-Bandgap Ferromagnetic Oxide. *Adv. Funct. Mater*, Vol 28, pp. 1705657, 2018. https://doi.org/10.1002/adfm.201705657

[5] J. Wang, Y. Li, L. Deng, N. Wei, Y. Weng, S. Dong, D. Qi, J. Qiu, X. Chen and T. Wu. High-Performance Photothermal Conversion of Narrow-Bandgap Ti_2O_3 Nanoparticles. *Adv. Mater*, Vol 29, pp. 603730, 2017. https://doi.org/10.1002/adma.201603730

[6] R. E. Newnhan and Y. M. de Haan. Refinement of the α-$A1_2O_3$, Ti_2O_3, V_2O_3 and Cr_2O_3 structures. *Z. Krista*, Vol 117, pp. 235-237, 1962. https://doi.org/10.1524/zkri.1962.117.2-3.235

[7] C. E. Rice and W. R. Robinson. High-temperature crystal chemistry of Ti_2O_3: structural changes accompanying the semiconductor-metal transition. *Acta Cryst*, Vol B33, pp. 1342-1348, 1977. https://doi.org/10.1107/S0567740877006062

[8] V. Singh and J. J. Pulikkotil. Electronic phase transition and transport properties of Ti_2O_3. *J. Alloy and Compounds*, Vol 658, pp. 430-434, 2016. https://doi.org/10.1016/j.jallcom.2015.10.203

[9] X. Zhong, J. Wang, S. Zhang, G. Yang and Y. Wang, Y. Ten-fold coordinated polymorph and metallization of TiO_2 under high pressure. *RSC Adv*, Vol 5, pp. 54253-54257, 2015. https://doi.org/10.1039/C5RA07245J

[10] X. Zhong, L. Yang, X. Qu, Y. Wang, J. Yang and Y. Ma. Crystal Structures and Electronic Properties of Oxygen-rich Titanium Oxides at High Pressure. *Inorg. Chem*, Vol 57, pp. 3254–3260, 2018. https://doi.org/10.1021/acs.inorgchem.7b03263

[11] Bruker (2006). APEX2, SAINT, Bruker AXS Inc., Madison, Wisconsin, USA 2006.

[12] G. M. Sheldrick. Program for the refinement of crystal structures. SADABS, Bruker AXS Inc., Madison, Wisconsin, USA 2002. http://shelx.uni-ac.gwdg.de/shelx/

[13] L. Palatinus and G. Chapuis. SUPERFLIP-a computer program for the solution of crystal structures by charge flipping in arbitrary dimensions. *Journal of Applied Crystallography*, Vol 40, pp. 786-790, 2007. https://doi.org/10.1107/S0021889807029238

[14] V. Petříček, M. Dušék and L. Palatinus. The crystallographic computing system. JANA, 2006 Institute of Physics, Praha, Czech Republic, 2006. www-xray.fzu.cz

[15] A. J. Clark, M. D. Segall, C. J. Pickard, P. J. Hasnip, M. I. Probert, K. Refson and M. C. Payne. First principles methods using CASTEP. *Z Krist Cryst Mater*, Vol 220, pp. 22567-22570, 2000. https://doi.org/10.1542/zkri.220.5.567.65075

[16] Materials Studio CASTEP Manual © Accelrys, 2010. http://www.tcm.phy.cam.ac.uk/castep/documentation/WebHelp/CASTEP.html.

[17] B. Hammer, L. B. Hansen and J. K.. Nørskov. improved adsorption energetic within density-functional theory using revised Perdew-Burke-Ernzerhof functionals. *Phys Rev*, Vol B59, pp. 7413-7421, 1999. https://doi.org/10.1103/PhysRevB.59.7413

[18] J. P. Perdew, K. Burke and M. Ernzerhof. Generalized Gradient Approximation Made Simple. *Phys. Rev. Lett*, Vol 77, pp. 3865-3868, 1996. https://doi.org/10.1103/PhysRevLett.77.3865

[19] C. E. Rise and W. R. Robinson. Structural changes in the solid solution $(Ti_{1-x}V_x)_2O_3$ as x varies from zero to one. *J. Solid State Chem*, Vol 21, pp. 145-154, 1977. https://doi.org/10.1016/0022-4596(77)90154-2

[20] C. E. Rise and W. R. Robinson. Structural changes resulting from doping Ti_2O_3 with Sc_2O_3 or Al_2O_3. *J. Solid State Chem*, Vol 15, pp. 155-160, 1977. https://doi.org/10.1016/0022-4596(77)90155-4

[21] W. R. Robinson. The crystal structures of Ti_2O_3, a semiconductor, and $(Ti_{0.900}V_{0.100})_2O_3$, a semimetal. *J. Solid State Chem*, Vol 9, pp. 255-260, 1974. https://doi.org/10.1016/0022-4596(74)90082-6

[22] L. M. Su, X. Fan, G. M. Cai and Z. P. Jin, Z.P. A peculiar layered 12-fold cationic coordination compound $LiInTi_2O_6$: phase relations, crystal structure and color-tunable photoluminescence. *RSC Adv*, Vol 7, pp. 22156-22169, 2017. https://doi.org/10.1039/c7ra01891f

[23] (a) I. D. Brown and D. Altermatt. Bond-valence parameters obtained from a systematic analysis of the Inorganic Crystal Structure Database. *Acta Cryst*, Vol B41, pp. 244-247, 1985. https://doi.org/10.1107/S0108768185002063

[24] Y. Le Page and P. Strobel. Structural chemistry of Magnéli phases Ti_nO_{2n-1} $(4 \le n \le 9)$. III. Valence ordering of titanium in Ti_6O_{11} at 130 K. *J. Solid State Chem*, Vol 47, pp. 6-15, 1983. https://doi.org/10.1016/0022-4596(83)90034-8

[25] L. F. Mattheiss. Electronic structure of rhombohedral Ti_2O_3. *J. Phys.: Condens. Matter*, Vol 8, pp. 5987-5995, 1996. https://doi.org/10.1088/0953-8984/8/33/007

[26] H. J. Zeiger. Unified model of the insulator-metal transition in Ti_2O_3 and the high-temperature transitions in V_2O_3. *Phys. Rev*, Vol B11, pp. 5132-5144, 1975. https://doi.org/10.1103/PhysRevB.11.5132

[27] Z. Hu and H. Metiu. Choice of U for DFT+U Calculations for Titanium Oxides. *J. Phys. Chem*, C, Vol 115, pp. 5841-5845, 2011. https://doi.org/10.1021/jp111350u

[28] S. H. Shin, G. V. Chandrashekhar, R. E. Loehman and J. M.Honig. Thermoelectric Effects in Pure and V-Doped Ti_2O_3 Single Crystals. *Phys. Rev*, Vol B8, pp. 1364-1372, 1973. https://doi.org/10.1103/PhysRevB.8.1364